J Mater Sci: Mater Med (2011) 22:1599–1606
DOI 10.1007/s10856-011-4322-7

Direct and interactive effects of three variables on properties of PMMA bone cement for vertebral body augmentation

Alejandro López · Erik Unosson · Håkan Engqvist · Cecilia Persson

Received: 20 October 2010 / Accepted: 11 April 2011 / Published online: 28 April 2011

Abstract PMMA bone cements are widely used for vertebral body augmentation procedures vertebroplasty and balloon kyphoplasty. Although there are studies in the literature on the direct effects of relevant variables on the properties of these cements, there are none on the interactive effects. In the present work, such a study was performed on both types of effects, with the variables being the concentration of initiator (benzoyl peroxide), the concentration of crosslinker (ethylene glycol dimethacrylate), and the liquid-to-powder ratio used in preparing the cement; and the properties being the compressive strength, the compressive modulus, the doughing time, the setting time, and the maximum polymerization temperature. Two additional properties obtained from the viscosity-versus-time curves, namely the time at the onset of curing, and the critical curing rate were also studied. Significant interactive effects between the amount of crosslinker and the amount of radical initiator were found to affect the doughing time and the critical curing rate. These effects were explained in terms of the reaction kinetics. It was concluded that interactive effects may exist and should be taken into account when designing bone cement formulations.

1 Introduction

Currently, two types of poly(methyl methacrylate) (PMMA)-based bone cements are commercially available for clinical use in vertebroplasty (VP) and balloon kyphoplasty (BKP). The first are brands approved by regulatory bodies (e.g., the US Food and Drug Administration, FDA) for anchoring total joint replacements (TJRs) [1, 2] (e.g., Surgical Simplex P), whose radiopacifier content is insufficient for VP and BKP. Therefore, additional amounts of the already present radiopacifier (e.g., $BaSO_4$ in Surgical Simplex P), or a different radiopacifier (e.g., Ta powder) are added by the surgeon/nurse until the radiopacifier content is in the order of 25–30 wt%. The second type of PMMA-based cements includes brands approved by regulatory bodies for use in VP and BKP [3, 4], e.g., KyphX HV-R, which contains 30 wt% $BaSO_4$ in the powder. At present, there is a growing literature regarding the effect of intrinsic variables (e.g., cement composition), and extrinsic variables (e.g., liquid-to-powder ratio (L/P)) on the properties of bone cements for VP and BKP [5–12]. Hernández et al. [11] compared the influence of $BaSO_4$ and bismuth salicylate radiopacifiers on the compressive strength, Young's modulus, doughing time, and setting time, among other properties. In general, these properties were not significantly affected by the amount and type of radiopacifier and their values satisfied the ISO 5833 (1992) standard. Lewis et al. [12] studied the influence of L/P on the polymerization rate and fatigue life of an iodine-containing bone cement, and concluded that there was a significant decrease of the polymerization rate when increasing L/P. Other related investigations that are reported in the literature are the influence of oscillatory mixing on injectability [5], and the effect of hyaluronic acid on the cement Young's modulus [13]. However, these studies are focused on the direct effect of such variables while ignoring possible interactive effects on the final properties of the cements. Furthermore, there is a lack of studies related to the effects of benzoyl peroxide (radical initiator), and ethylene glycol dimethacrylate, on the properties of PMMA bone cements for VP and BKP.

A. López · E. Unosson · H. Engqvist · C. Persson (✉)
Department of Engineering Sciences, Division of Applied Materials Science, The Ångström Laboratory, Uppsala University, Uppsala, Sweden
e-mail: cecilia.persson@angstrom.uu.se

Design-of-experiments (DOE) software packages are widely available and are used for, among other things, screening of process factors, process optimization and robustness testing [14]. The aim of screening is to investigate which factors affect the responses of interest; optimization is to obtain information on how these factors combine to affect the responses; robustness testing is to determine how small fluctuations in the factors affect the responses.

The purpose of the present study was to screen the direct and interactive effects of three variables on six properties of a PMMA bone cement formulation that may be used for VP and BKP. The variables were the concentration of a radical initiator (benzoyl peroxide) (BPO) in the powder, the concentration of a crosslinker (ethylene glycol dimethacrylate) (EGDMA) in the liquid, and the liquid-to-powder ratio (L/P) used to prepare the cement. The properties of interest were the compressive strength (σ_{max}), the compressive modulus (E), the doughing time (t_{dough}), the setting time ($t_{setting}$), the maximum polymerization temperature (T_{max}), and the change of the complex viscosity (η^*) over time. The last was described in terms of the time at the onset of cure (t_{ons}) and the critical cure rate (CCR).

2 Materials

Nine experimental formulations were synthesized in our laboratory. In each of these formulations, the powder phase was composed of PMMA beads with mean average molecular weight = 350 kDa, and mean particle size = 95 μm, as measured using laser scattering granulometer (Mastersizer X; Malvern Instruments Ltd., Malvern, UK); benzoyl peroxide; and 30 wt% barium sulphate ($BaSO_4$). The liquid phase was composed of methyl methacrylate (MMA); a peroxide decomposer, *N*,*N*-dimethyl-*p*-toluidine (DMPT); and a crosslinker (EGDMA). The amounts are shown in Table 1. The concentration of DMPT was maintained equimolar to that of BPO since this has been shown to be the optimal activator-to-initiator ratio, in the case of PMMA bone cements for anchoring TJRs [15]. All of the chemicals were purchased from Sigma–Aldrich (St. Louis, MO, USA) and used as received.

Table 1 Full factorial experimental design including three variables: [BPO], [EGDMA] and L/P

Sample ID	[BPO] (wt%)	[EGDMA] (vol%)	L/P (ml/g)
N1	1	0	0.6
N2	1	0	0.8
N3	1	10	0.6
N4	1	10	0.8
N5	3	0	0.6
N6	3	0	0.8
N7	3	10	0.6
N8	3	10	0.8
N9	2	5	0.7

3 Methods

3.1 Experimental design

Experimental formulations with the three variables being the concentration of BPO [BPO], the concentration of EGDMA [EGDMA], and L/P (Table 1), were prepared. Experiments were performed around the center-point of [BPO] = 2 wt%, [EGDMA] = 5 vol%, and L/P = 0.7 ml/g. The center-point was chosen as follows: [BPO] and L/P based on the literature [4, 16], and preliminary experiments that indicated that [BPO] = 2 wt%, and L/P = 0.7 ml/g gave cements with good handling characteristics using the reagents specified in the materials section; [EGMDA] = 5 vol% is similar to 4.28 vol% as used in Vertebroplastic® (DePuy Acromed, Inc. Raynham, MA, USA), and the effect of such amount on bone cements for TJR has been reported in the literature [17]. A screening step was performed using a two-level full factorial design (Table 1) and a polynomial interaction model fitted with partial least squares (PLS). The model thus had the following equation:

$$y = \beta_0 + \beta_1 x_1 + \beta_2 x_2 + \beta_3 x_3 + \beta_{12} x_1 x_2 + \beta_{13} x_1 x_3 + \beta_{23} x_2 x_3 + \varepsilon \quad (1)$$

3.2 Preparation of the cement

The powder constituents were thoroughly mixed by hand in a glass mortar with a glass pestle. A timer was started when the liquid was added to the powder. A thermocouple was used to register the ambient temperature. The liquid and the powder were mixed with a metal spatula for 1 min and then 1 ml was extracted with a polypropylene syringe for the rheometry. The rest of the mixture was let to sit for 30 s and then mixed for another 10 s before the specimens for the compressive strength test were prepared. The remainder of the mixture was used to determine t_{dough}, $t_{setting}$, and T_{max}.

3.3 Compression tests

After approximately 100 s from the start of the mixing, the dough was injected into Teflon® moulds using 1 ml polypropylene syringes to produce samples of 6 mm diameter and 12 mm height as stipulated in ASTM F451-08 [18]. The cured specimens were conditioned for 24 h in ambient laboratory conditions (T = 21 ± 1°C), and then tested

using a universal materials testing machine (AGS-H; Shimadzu, Kyoto, Japan) at a crosshead displacement rate of 25.4 mm/min. From the force-versus-displacement curves, σ_{max}, and E were obtained.

3.4 Handling and thermal properties

The t_{dough} was determined as the time at which freshly-exposed cement separated cleanly from a powder-free nitrile glove dipped into the dough. After t_{dough} was determined, approximately 25 g of the dough was placed into a Teflon® mould, after which a plot of dough temperature-versus-time during curing was obtained. Then $t_{setting}$, and T_{max} were determined from this plot [18].

3.5 Rheometry

The evolution of the cement viscosity during cement curing was determined in the form of complex viscosity-versus-time (η^*–t) curve from commencement of mixing using a stress-controlled rheometer (AR2000; TA instruments, New Castle, DE, USA), equipped with a parallel-plate geometry, in a time-sweep step-mode, at a constant frequency of 5 Hz. The upper plate was a 19 mm diameter titanium plate and the gap was kept at 2000 μm [19]. The displacement amplitude was 5×10^{-4} rad and the temperature of the lower plate was maintained at 23°C [19].

3.6 Statistical analysis

A DOE software package (MODDE; Umetrics AB, Umeå, Sweden), was used to produce predictive graphs based on a two-level full factorial (2^3) design with an interaction model fitted using the PLS method. The parameters whose contribution to a specified response (material property) was considered statistically insignificant were those whose confidence interval included zero. In the first step, the coefficients for all the responses including every output parameter were determined. The model was then refitted excluding statistically insignificant parameters. For the PLS, the following parameters were obtained: the goodness of fit (R^2), the goodness of prediction (Q^2), the model validity, and the reproducibility. The model validity measures if the chosen model is appropriate in a general sense and values above 0.25 suggest a valid model [14]. The reproducibility represents the replicate error in relation to the variability across the design and values above 0.5 indicate good control over the experimental procedure [14]. Analysis-of-variance (ANOVA) was also performed on the regression using MODDE, with significance denoted at $P < 0.05$.

4 Results

4.1 Compressive and curing properties

A summary of these properties is given in Tables 2, 3.

4.2 Rheometry

Typical η^*–t curves are given in Fig. 1. These results were analyzed using two parameters, namely, time at the onset of cure (t_{ons}) and the critical cure rate (CCR). Lewis and Carroll [20] defined t_{ons} as the time when η^* increases sharply and CCR as the slope of the η^*–t curve at t_{ons}. In the present work, however, t_{ons} was defined as the time when η^* reached 250 Pa s. The reason for this is that in formulations where [EGDMA] = 0 vol%, the curves increased smoothly with time. For each of the other formulations, it was observed that η^* increased rapidly with t when $\eta^* = 250$ Pa s was achieved. Thus CCR was calculated as the slope of the η^*–t curve at $\eta^* = 250$ Pa s. A summary of the t_{ons} and CCR results is given in Table 4.

Table 2 Summary of the compressive properties

Batch ID	N	σ_{max} MPa (mean ± SD)	E MPa (mean ± SD)
N1	15	77.1 ± 15.1	1158.1 ± 238.3
N2	15	70.8 ± 9.0	957.6 ± 229.4
N3	25	94.9 ± 8.1	1258.0 ± 175.4
N4	17	89.7 ± 11.4	1253.15 ± 116.7
N5	20	76.5 ± 9.9	1231.2 ± 99.2
N6	19	72.8 ± 11.9	1150.3 ± 311.8
N7	12	99.4 ± 4.9	1277.5 ± 119.2
N8	12	99.7 ± 7.7	1176.5 ± 282.8
N9	21	95.2 ± 7.0	1236.9 ± 169.2

Table 3 Summary of the curing and thermal properties

Batch ID	N	T_o^a (°C)	t_{dough} (min)	$t_{setting}$ (min)	T_{max} (°C)
N1	3	21.1 ± 1.3	31.1 ± 3.9	49.3 ± 13.7	33.4 ± 7.1
N2	3	23.3 ± 0.3	36.2 ± 5.6	57.0 ± 12.8	46.7 ± 8.1
N3	4	20.9 ± 0.9	15.3 ± 1.9	24.1 ± 1.2	53.5 ± 10.4
N4	4	22.9 ± 1.8	17.7 ± 2.6	26.5 ± 5.5	75.6 ± 15.9
N5	4	20.9 ± 0.9	10.6 ± 2.6	18.3 ± 3.3	39.6 ± 8.5
N6	4	22.1 ± 1.6	14.0 ± 3.2	20.0 ± 4.7	46.5 ± 11.2
N7	3	22.7 ± 1.8	5.3 ± 0.4	6.8 ± 0.9	55.1 ± 12.6
N8	3	21.8 ± 2.8	7.0 ± 1.1	7.8 ± 1.6	89.6 ± 24.0
N9	3	21.1 ± 0.2	13.5 ± 0.9	19.1 ± 0.7	49.1 ± 3.3

[a] Room temperature as measured with a thermocouple just before the dough was placed into the standard Teflon® mould

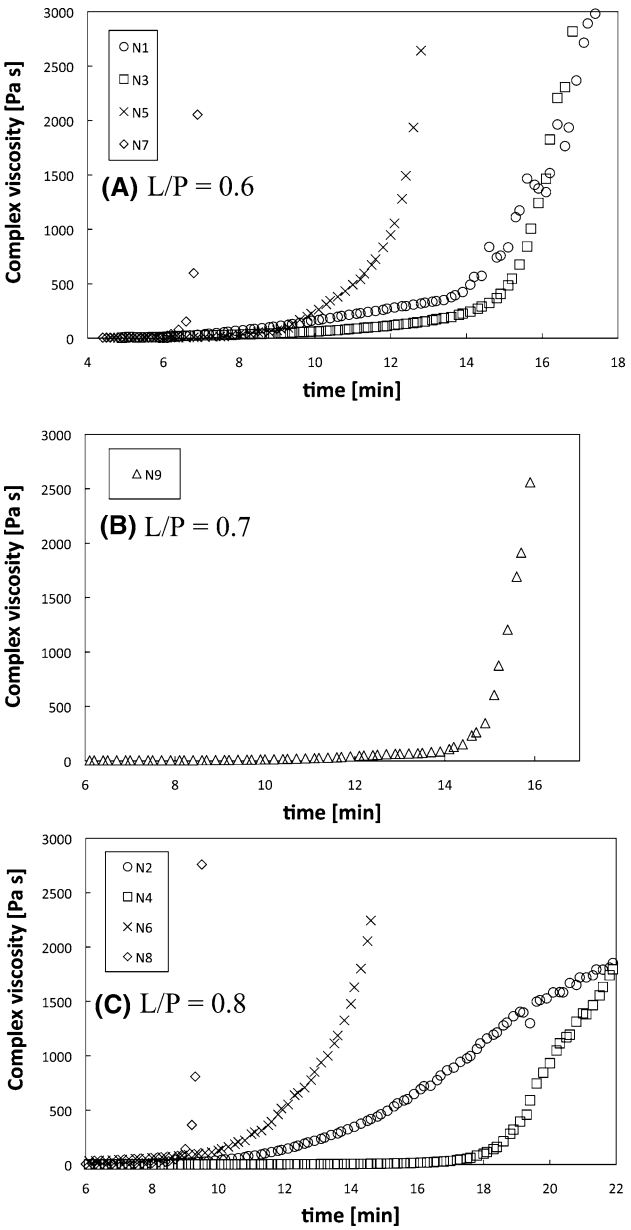

Fig. 1 Typical η^*–t curves

4.3 Statistical analysis

The regression coefficients and the results for the polynomial model that was used for screening after refitting are given in Table 5. It is realized that the scaled and centered coefficients illustrate the importance of each parameter, however, for practical purposes the unscaled coefficients are also given. The predictive responses (material properties) after refitting are presented in Fig. 2. The results (Table 5 and Fig. 2) show that (1) there were significant direct effects, namely, [EGDMA] on σ_{max}; [BPO] and [EGDMA] on $t_{setting}$; L/P and [EGDMA] on T_{max}, and (2) there were two significant interactive effects, namely, [BPO] and [EGDMA] on both t_{dough} and CCR.

5 Discussion

The increasing literature on the (direct) effects of intrinsic and extrinsic variables on the properties of PMMA bone cement, often disregards possible interactive effects. Therefore, this study aimed to screen the direct as well as the interactive effects of three variables, i.e., [BPO], [EGDMA], and L/P on eight responses (material properties), i.e., σ_{max}, E, t_{dough}, $t_{setting}$, T_{max}, t_{ons}, and CCR using MODDE, a DOE software package.

Crosslinking agents such as dimethacrylates are commonly included in formulations for TJR, in order to form anchoring points, and stiffer networks that shrink to a smaller extent [2]. They have also been included in commercial formulations for VP, namely, Vertebroplastic® (DePuy Acromed, Inc. Raynham, MA, USA), with 4.28 vol% EGDMA; and Cortoss® (Orthovita, Inc. Malvern, PA, USA), a composite containing a mixture of different monomers (59 vol%), including triethylene glycol dimethacrylate (TEGDMA) [4]. Previous investigations report that (1) there is a general trend of reduced reactivity, and a higher propensity to intramolecular cyclization, as the number of ethylene glycol units increases for free-radical polymerizations involving mono-, di-, and TEGDMA [21]; (2) increasing the number of ethylene glycol units does not appreciably increase the tensile strength and lowers the strain at maximum stress [17]; (3) Dimethacrylates generally improve the tensile strength and reduce the brittleness of $BaSO_4$-containing bone cements for TJR [22]. Given the above and the fact that cements for VP or BKP differ from those intended for TJR mainly in their concentration of radiopacifier, the variable [EGDMA] was selected as a relevant variable for this study.

Some of the problems associated with VP may be due to inadequate values of the properties herein investigated. Standard bone cement for VP has a relatively high E between 1.5 and 3.5 GPa [9, 23, 24] compared to the surrounding bone, which has been hypothesized to contribute to additional, adjacent fractures [25]. Thus, an E more similar to that of the surrounding bone may be more adequate for bone cements used in the spine (E = 0.05–0.8 GPa in cancellous bone [23]). The σ_{max} of the cement should at least be higher than that of cancellous bone, which is between 1 and 15 MPa [9] (a minimum value of 70 MPa as stipulated by ASTM F451-08 is commonly referred to, since there is no standard specification for bone cements for VP). The t_{dough} can be used as an indication of the maximum injection time since VP cements are not used in the dough state. The $t_{setting}$ is an

Table 4 Summary of the t_{ons} and CCR results

Batch ID	t_{ons} (min)	CCR (Pa s/min)
N1	11.6	54.0
	6.0	106.0
N2	9.3	178.0
	13.2	119.0
N3	13.9	132.5
	N/A	N/A
N4	16.1	151.0
	18.7	340.5
N5	14.7	287.5
	10.0	184.5
N6	10.9	284.5
	18.0	244.0
N7	8.7	579.0
	6.6	2218.0
N8	9.1	1103.0
	10.5	1140.5
N9	14.5	234.0
	14.7	291.0
	10.9	670.0
	14.7	630.0

indication of how long time it would take for the dough to become a solid material of maximum strength, which is of interest for the clinicians. Temperatures above 50°C for more than 1 min may be detrimental for bone tissues [26, 27], and therefore, the reduction of T_{max} is desired in order to diminish any thermal damage inside the vertebral body or the tissues around it. Finally, knowledge of the change of viscosity over time is important to avoid cement leakage in VP [10, 19, 28].

The change of η^* with time plays an important role when designing bone cements for VP. A previous study [10] has suggested that in order to avoid cement leakage, the cement should have an initial viscosity of 100 Pa s, and stay below 200 Pa s for a considerable period of time before final curing, to allow enough time for the surgeon to inject the material. All η^*–t curves in Fig. 1 exhibited similar behavior, including an initial period of low viscosity, which is generally desired for cements to be used in VP. This was followed by a period of slow increase of η^*, which was shorter for N7 and N8, which had a high [EGDMA], and [BPO]. This is due to a higher concentration of growing radicals, which may increase the overall polymerization rate. Finally, when t_{ons} was reached, the viscosity increased exponentially.

After the statistical analysis, the following trends were found: (a) σ_{max} increases significantly with [EGDMA]; (b) t_{dough} decreases significantly with [EGDMA] and [BPO], with a significant interactive effect; (c) $t_{setting}$ decreases significantly with [EGDMA] and [BPO] with insignificant interactive effect; (d) T_{max} increases significantly with [EGDMA] and L/P with insignificant interactive effect; (e) CCR increases significantly with [EGDMA] and [BPO], with a significant interactive effect. The increase of σ_{max} with [EGDMA] may be due to a higher crosslinking density. Similar trends were observed for

Table 5 Responses and their corresponding regression coefficients: unscaled (above) and scaled (below), for the polynomial interaction model

y	β_0	β_1 (L/P)	β_2 (EGDMA)	β_3 (BPO)	β_{23} (EGDMA*BPO)	R^2	Q^2	Val.	Rep.	P
σ_{max}	76.75		2.16							
	–	NS	–	NS	NS	0.72	0.68	0.897	0.622	0.001
	87.56		9.67							
E	NS	NS	NS	NS	NS	–	–	–	–	–
T_{max}	−27.27	96.00	2.69							
	–	–	–	NS	NS	0.85	0.76	0.547	0.957	0.000
	53.38	8.59	12.03							
t_{dough}	43.33		−2.27	−10.68	0.55					
	–	NS	–	–	–	0.92	0.72	0.210	0.993	0.000
	16.15		−5.21	−7.09	−2.20					
t_{set}	60.28		−1.99	−13.00						
	–	NS	–	–	NS	0.89	0.84	0.071	0.995	0.000
	24.35		−8.88	−11.63						
t_{ons}	NS	NS	NS	NS	NS	–	–	–	–	–
CCR	27.66		−39.27	67.94	46.76					
	–	NS	–	–	–	0.80	0.71	0.914	0.660	0.000
	434.75		242.87	269.87	187.03					

NS not significant, *Val.* validity; *Rep.* reproducibility

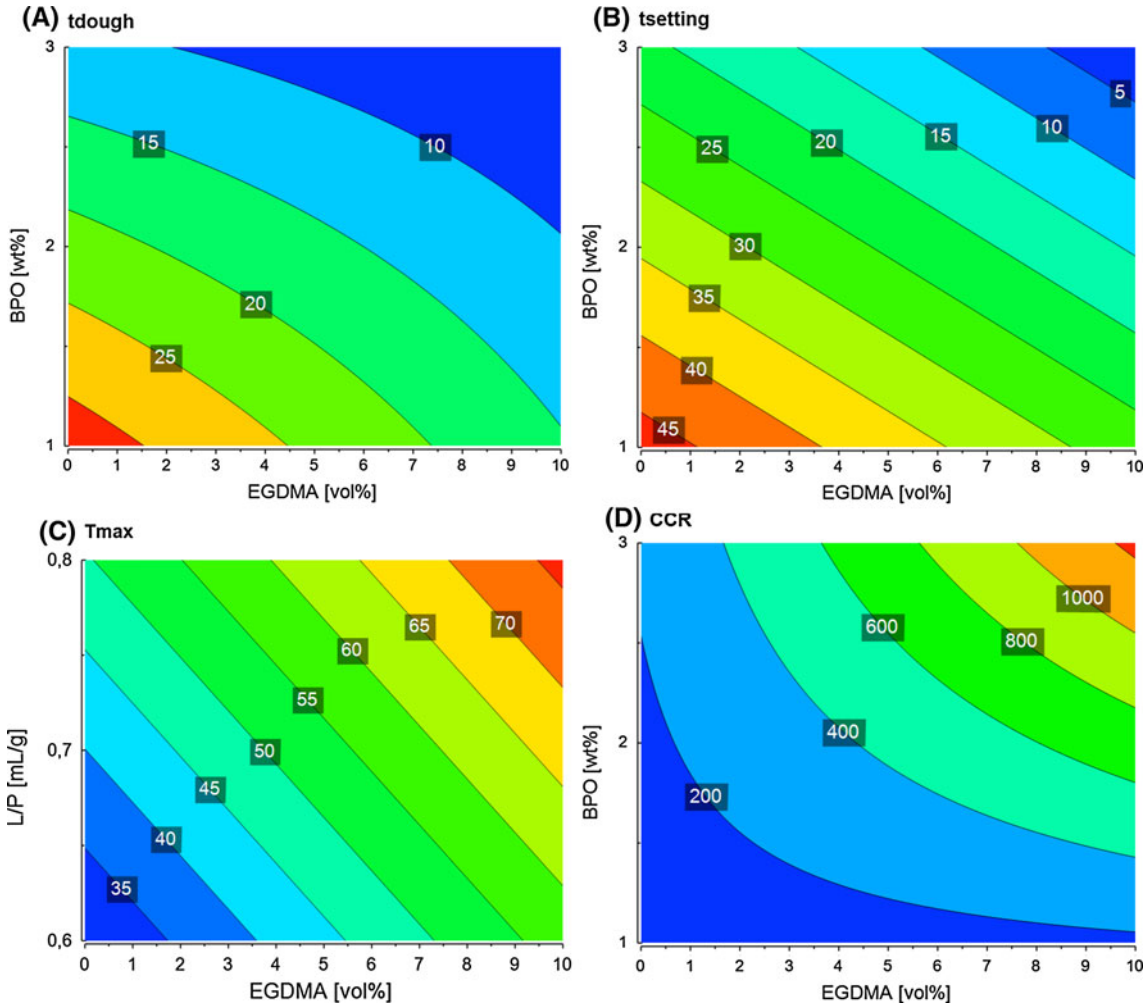

Fig. 2 Predictive charts showing the responses to correspondent significant parameters after the models were re-fitted using MODDE: **a** t_{dough} depends on the interactive effect between [BPO] and [EGDMA]; **b** $t_{setting}$ depends on [BPO] and [EGDMA]; **c** T_{max} depends on L/P and [EGDMA]; **d** CCR depends on the interactive effect between [BPO] and [EGDMA]

t_{dough} and $t_{setting}$, which decreased with: (1) [EGDMA] due to a faster network formation (EGDMA is a bifunctional monomer); (2) [BPO] due to a higher concentration of phenyl radicals that can attack the vinyl group in MMA or EGDMA [16]. Importantly, an interactive effect of [EGDMA] and [BPO] was found to significantly affect the t_{dough}. This is indicated by the non-linearity of the isochronal curves in Fig. 2a and its regression coefficients shown in Table 5. Since [EGDMA] and [BPO] interact, the relation between each of these variables and t_{dough} (dependant variable) will depend on the other. Accordingly, it is observed that at higher [BPO], the t_{dough} is lower regardless of [EGDMA] whereas at lower [BPO] the t_{dough} is more dependant on [EGDMA]. This could be explained through the reaction kinetics. A typical free-radical polymerization is characterized by a rapid increase in molecular weight, and subsequent auto-acceleration (gel effect) early in the reaction [21, 29]. This effect is mainly enhanced by (1) a higher presence of active radicals, which depends on [BPO], and (2) a reduction in chain mobility due to the crosslinking, which in turn, depends on [BPO] and [EGDMA]. Therefore, at higher [BPO] the onset of the auto-acceleration occurs earlier and the reaction is faster due to a higher number of initiating radicals. On the other hand, at lower [BPO], the auto-acceleration occurs earlier due to more restricted chain mobility when increasing [EGDMA]. T_{max} was found to increase with [EGDMA], which could be because of a lower heat dissipation capacity [17] due to a denser network. The same trend was observed when increasing L/P, which might be due to the higher amount of monomer available, resulting in more exothermic reactions taking place [30]. Finally CCR was found to be significantly affected by the interactive effect of [EGDMA] and [BPO]. From the models, it was observed that CCR increased when increasing both [BPO], and [EGDMA] simultaneously. However, at low values of [EGDMA], low

values of CCR were observed independently of the [BPO]. The reaction rate-versus-time curves for free-radical crosslinking of MMA and EGDMA in the presence of 2,5-dimethyl-2,5-bis((2-ethylhexanoyl)peroxy)hexane are reported in the literature [31]. From here, it is seen that when [EGDMA] $\leq$ 20 wt%, the reaction is initially kinetic-controlled (i.e., indicated by a plateau), and then followed by auto-acceleration [31]. Moreover, the plateau becomes shorter, and the peak reaction rate increases as the amount of EGDMA increases with respect to that of MMA [31]. This correlates with the fact CCR increased with [EGDMA] at constant BPO (Fig. 2e). However, the effect of BPO on the kinetics of free-radical crosslinking of a system containing PMMA, MMA and EGDMA remains to be assessed. More importantly, the results indicated that regardless of the monomer content, the curing profiles of PMMA bone cement can be controlled by means of the interactive effect between [EGDMA] and [BPO].

One limitation of this study is the use of ASTM F451-08 standard, as this standard is intended for bone cements to be used in TJR. However, both ASTM F451-08 and ISO 5833 are widely referred to in the literature, regardless of the type of the cement, as there is currently no standard specification for acrylic cements for VP [4]. Another limitation is the use of a first order polynomial model to describe y (material property) as a function of the independent variables [BPO], [EGDMA], and L/P. This type of model is adequate for screening purposes, but a quadratic model may be of interest for further optimization. Also, the limits established here for the independent variables may not capture all formulations of interest. These limits were based on the literature as well as preliminary experiments around the center-point formulation. Those experiments showed that outside these limits, the cements had problems with their setting characteristics.

6 Conclusions

The direct and interactive effects of [BPO], [EGDMA], and L/P on the PMMA bone cement properties σ_{max}, E, t_{dough}, $t_{setting}$, T_{max}, t_{ons}, and CCR were screened using MODDE, a DOE software package. Contour maps, which were based on an interaction polynomial model fitted with PLS, were successfully generated. The unscaled and scaled regression coefficients were also obtained. The results showed that: (1) There were significant direct effects, namely, [EGDMA] on σ_{max}, [EGDMA] and [BPO] on $t_{setting}$, and [EGDMA] and L/P on T_{max}; (2) There were significant interactive effects between [EGDMA] and [BPO] on both t_{dough} and CCR; (3) E and t_{ons} were not affected significantly by any of the variables studied here. The interactive effects could be explained in terms of the reaction kinetics. It was concluded that the concentrations of BPO and EGDMA have an important role in controlling the final properties of PMMA bone cements and could be useful for tailoring the cement curing profiles.

In conclusion, the evaluation of the interactive effects, in addition to the direct effects, was found to be useful for the understanding and the prediction of the behavior of complex systems such as bone cements, in which several intrinsic and extrinsic variables have a simultaneous influence on the curing and the final properties.

Acknowledgments Funding from the European Union for The Osteoporotic Virtual Physiological Human project (VPHOP FP7-ICT2008-223865) is gratefully acknowledged. We acknowledge Janne Bohlin from the Division of Polymer Chemistry at Uppsala University for the technical assistance in the use of the stress-controlled rheometer.

References

1. Lewis G. Properties of acrylic bone cement: state of the art review. J Biomed Mater Res. 1997;38(2):155–82.
2. Lewis G. Alternative acrylic bone cement formulations for cemented arthroplasties: present status, key issues, and future prospects. J Biomed Mater Res B. 2008;84B(2):301–19.
3. Lieberman IH, Togawa D, Kayanja MM. Vertebroplasty and kyphoplasty: filler materials. Spine J. 2005;5(6, Supplement 1):S305–16.
4. Lewis G. Injectable bone cements for use in vertebroplasty and kyphoplasty: state-of-the-art review. J Biomed Mater Res B. 2006;76B(2):456–68.
5. Baroud G, Matsushita C, Samara M, Beckman L, Steffen T. Influence of oscillatory mixing on the injectability of three acrylic and two calcium-phosphate bone cements for vertebroplasty. J Biomed Mater Res B. 2004;68B(1):105–11.
6. Race A, Mann KA, Edidin AA. Mechanics of bone/PMMA composite structures: an in vitro study of human vertebrae. J Biomech. 2007;40(5):1002–10.
7. Hernández L, Vázquez B, López-Bravo A, Parra J, Goñi I, Gurruchaga M. Acrylic bone cements with bismuth salicylate: behavior in simulated physiological conditions. J Biomed Mater Res A. 2007;80A(2):321–32.
8. Boger A, Bohner M, Heini P, Verrier S, Schneider E. Properties of an injectable low modulus PMMA bone cement for osteoporotic bone. J Biomed Mater Res B. 2008;86B(2):474–82.
9. Boger A, Bisig A, Bohner M, Heini P, Schneider E. Variation of the mechanical properties of PMMA to suit osteoporotic cancellous bone. J Biomater Sci Polym Ed. 2008;19:1125–42.
10. Loeffel M, Ferguson SJ, Nolte L-P, Kowal JH. Vertebroplasty: experimental characterization of polymethylmethacrylate bone cement spreading as a function of viscosity, bone porosity, and flow rate. Spine. 2008;33(12):1352–9. doi:10.1097/BRS.0b013e3181732aa9.
11. Hernández L, Gurruchaga M, Goñi I. Injectable acrylic bone cements for vertebroplasty based on a radiopaque hydroxyapatite. Formulation and rheological behaviour. J Mater Sci Mater Med. 2009;20(1):89–97.
12. Lewis G, Koole LH, van Hooy-Corstjens CSJ. Influence of powder-to-liquid monomer ratio on properties of an injectable iodine-containing acrylic bone cement for vertebroplasty and balloon kyphoplasty. J Biomed Mater Res B. 2009;91B(2):537–44.

13. Boger A, Bohner M, Heini P, Schwieger K, Schneider E. Performance of vertebral cancellous bone augmented with compliant PMMA under dynamic loads. Acta Biomater. 2008;4(6):1688–93.
14. Eriksson L, Johansson E, Kettaneh-Wold N, Wikström C, Wold S. Design of experiments: principles and applications. Umeå: Umetrics; 2008.
15. Madigan S, Towler M, Lewis G. Optimisation of the composition of an acrylic bone cement: application to relative amounts of the initiator and the activator/co-initiator in Surgical Simplex® P. J Mater Sci Mater Med. 2006;17(4):307–11.
16. Nussbaum DA, Gailloud P, Murphy K. The chemistry of acrylic bone cements and implications for clinical use in image-guided therapy. J Vasc Interv Radiol. 2004;15(2):121–6.
17. Deb S, Braden M, Bonfield W. Effect of crosslinking agents on poly(ethylmethacrylate) bone cements. J Mater Sci Mater Med. 1997;8(12):829–33.
18. ASTM. F451, 2008, Standard specification for acrylic bone cement. West Conshohocken: ASTM International; 2008.
19. Farrar DF, Rose J. Rheological properties of PMMA bone cements during curing. Biomaterials. 2001;22(22):3005–13.
20. Lewis G, Carroll M. Rheological properties of acrylic bone cement during curing and the role of the size of the powder particles. J Biomed Mater Res. 2002;63(2):191–9.
21. Scranton AB, Bowman CN, Klier J, Peppas NA. Polymerization reaction dynamics of ethylene glycol methacrylates and dimethacrylates by calorimetry. Polymer. 1992;33(8):1683–9.
22. Deb S, Vazquez B. The effect of cross-linking agents on acrylic bone cements containing radiopacifiers. Biomaterials. 2001;22(15):2177–81.
23. Beck S, Boger A. Evaluation of the particle release of porous PMMA cements during curing. Acta Biomater. 2009;5(7):2503–7.
24. Hernandez L, Muñoz ME, Goñi I, Gurruchaga M. New injectable and radiopaque antibiotic loaded acrylic bone cements. J Biomed Mater Res B. 2008;87B(2):312–20.
25. Trout AT, Kallmes DF, Layton KF, Thielen KR, Hentz JG. Vertebral endplate fractures: an indicator of the abnormal forces generated in the spine after vertebroplasty. J Bone Miner Res. 2006;21(11):1797–802.
26. Eriksson RA, Albrektsson T. The effect of heat on bone regeneration: an experimental study in the rabbit using the bone growth chamber. J Oral Maxillofac Surg. 1984;42(11):705–11.
27. Eriksson RA, Albrektsson T, Magnusson B. Assessment of bone viability after heat trauma: a histological, histochemical and vital microscopic study in the rabbit. J Plast Reconstr Surg Hand Surg. 1984;18(3):261–8.
28. Nicholas MKD, Waters MGJ, Holford KM, Adusei G. Analysis of rheological properties of bone cements. J Mater Sci Mater Med. 2007;18(7):1407–12.
29. Yu Q, Zeng F, Zhu S. Atom transfer radical polymerization of poly(ethylene glycol) dimethacrylate. Macromolecules. 2001;34(6):1612–8.
30. Turner RC, Atkins PE, Ackley MA, Park JB. Molecular and macroscopic properties of PMMA bone cement: Free-radical generation and temperature change versus mixing ratio. J Biomed Mater Res. 1981;15(3):425–32.
31. Sun X, Chiu YY, Lee LJ. Microgel formation in the free radical cross-linking copolymerization of methyl methacrylate (MMA) and ethylene glycol dimethacrylate (EGDMA). Ind Eng Chem Res. 1997;36(4):1343–51.